UDC 004.93

ADAPTIVE PERONA–MALIK FILTERING FOR ULTRASOUND SPECKLE REDUCTION USING LOCAL ENTROPY

[1,2*]*Yusupov O.R.*, [2]*Olimjonova S.G.*, [2]*Badalova L.B.*

*ozodyusupov@gmail.com
[1]Samarkand State University named after Sharof Rashidov,
Samarkand, Uzbekistan.
[2]Digital technologies and artificial intelligence development research institute,
Tashkent, Uzbekistan

Abstract. This paper addresses speckle noise reduction in ultrasound (EchoKG) imaging, which strongly impacts diagnostic accuracy. An entropy-driven adaptive extension of the Perona–Malik anisotropic diffusion model is proposed, where the diffusion coefficient is controlled locally using entropy and variance. This enables stronger smoothing in homogeneous regions and reduced diffusion near edges and tissue boundaries, thus preserving anatomical structures. Experiments on echocardiographic B-scan images show that the method outperforms the classical Perona–Malik model by 3–4 dB in PSNR and 0.06 in SSIM, achieving a better balance between noise suppression and edge retention. The results indicate that the proposed entropy-based adaptive diffusion improves visual clarity, preserves myocardial and valve contours, and enhances diagnostic reliability. Overall, the method provides a robust and computationally efficient filtering framework for real-time medical imaging and intelligent diagnostic systems.

Keywords: ultrasound imaging, speckle noise, anisotropic diffusion, Perona–Malik model, entropy, adaptive filtering, medical image processing.

1 Introduction*

Heart failure is one of the most critical medical challenges currently facing global healthcare systems. According to recent epidemiological studies, approximately 56.2 million people worldwide are living with this disease. Heart failure is a chronic pathology characterized by impaired myocardial contractility, disrupted blood circulation, insufficient oxygen delivery to body tissues, and a consequent decline in quality of life [1, 2]. According to the World Health Organization (WHO), heart failure affects about 1–3% of the global population, and among individuals over 70 years of age, this figure exceeds 10% [3]. Each year, deaths associated with heart failure number around 9–10 million, representing a significant proportion of overall cardiovascular mortality.

In recent years, the integration of artificial intelligence (AI) and data-driven analytical algorithms into medical diagnostic systems has accelerated, with the goal of automating digital cardiac analysis, early diagnosis, and real-time condition monitoring [4, 5]. Echocardiographic (EchoKG) ultrasound imaging, in particular, stands out due to its noninvasive nature, real-time efficiency, and high clinical value in diagnosing cardiovascular disorders.

However, processing EchoKG images presents several technical challenges. One of the most prominent issues is *speckle noise*. This noise arises from the interference of coherent ultrasound waves reflected from biological tissues, resulting in random phase shifts and intensity fluctuations that appear as granular patterns in the image. Speckle noise not only degrades visual quality but also significantly reduces the accuracy of structural analysis, segmentation, and boundary detection tasks.

The mathematical model of a speckle-noised ultrasound image is expressed as:

$$I_0 = I + \sqrt{I}\, n, \tag{1}$$

where I represents the true (noise-free) image intensity, I_0 is the noisy image intensity, and n is zero-mean Gaussian noise with variance σ_n.

Ultrasound images acquired from diagnostic equipment usually undergo preliminary digital processing. One of these preprocessing steps is dynamic range compression, which adjusts the image for better visual perception by the human eye. The compression process is defined as:

$$\tilde{I} = \alpha \cdot \log(I_0 + 1) + \beta, \quad (2)$$

where α and β are parameters controlling contrast and brightness, respectively.

The inverse process (decompression) can be represented as:

$$I_0 = \exp(\tilde{I}) - 1. \quad (3)$$

Thus, preprocessed ultrasound images are prepared for subsequent analysis, edge detection, and diagnostic modeling. In this work, adaptive filtering approaches based on nonlinear diffusion models are investigated, with particular attention to an entropy-based adaptive modification of the Perona–Malik diffusion model for speckle noise reduction in echocardiographic images.

2 Literature review

In recent years, numerous approaches have been proposed to address the problem of speckle noise reduction and edge preservation in ultrasound imaging. Early studies widely utilized median filtering methods [6], which effectively suppress noise while preserving image structure, particularly fine interlayer boundaries. Subsequently, a two-dimensional weighted version of the Savitzky–Golay filter was developed to improve upon this approach [7]. By employing a polynomial smoothing mechanism that accounts for local linearity, this filter achieved better preservation of structural continuity.

The adaptive weighted median filter (AWMF) [8] operates in accordance with local statistical properties of the image. Filter weights are updated based on the local variance of each region, resulting in stronger smoothing in homogeneous areas and better preservation of structural details at high-contrast edges.

Wavelet-based approaches [9] play a significant role in ultrasound image denoising. Studies have shown that filtering performance is highly dependent on wavelet transform parameters, the type of ultrasound data, and noise level. Inappropriate parameter selection may lead to loss of important details or insufficient noise suppression; therefore, parameter tuning is often performed empirically.

More recently, deep learning-based techniques have been actively explored. For instance, the CycleGAN architecture [10] enables noise reduction while preserving image details by performing bidirectional domain mapping between noisy and clean data. However, model training instability, reduced accuracy in high-noise conditions, and substantial computational cost limit its applicability in real-time systems. The anisotropic diffusion approach [11] represents a classical framework that allows smoothing while preserving edges in ultrasound images. In this method, the diffusion rate varies as a function of the image gradient magnitude: smoothing is stronger in homogeneous regions and weaker near edges. Consequently, the model achieves an optimal balance between speckle suppression and structure preservation.

Approaches based on the Dual-Tree Complex Wavelet Transform (DTCWT) [12] improve directional sensitivity and phase accuracy compared to standard wavelet transforms. This transformation detects and suppresses noise based on local energy distribution while retaining texture and edge information. As a result, DTCWT achieves an effective trade-off between noise reduction and detail preservation. Among statistical modeling methods, Gaussian Process Regression (GPR) [13] has received considerable attention. In this approach, pixel intensities are modeled as random variables, and adaptive smoothing is performed based on correlations among them. Although GPR yields high denoising accuracy, its computational complexity limits real-time applicability. Kernel Ridge Regression (KRR) [14] performs nonlinear regression using kernel functions to map noisy pixel intensities to their corresponding noise-free signals. It produces results similar to those of GPR but with faster computation, making it more suitable for real-time medical systems.

The Optimized Modified Three-Step Search (O-MTSS) algorithm [15] achieves both noise reduction and detail preservation. By integrating kinematic clustering and hybrid search mechanisms,

this method provides significant improvements in real-time ultrasound imaging. However, due to possible errors during the initial stage, a slight degradation in accuracy can occasionally occur.

Furthermore, hybrid combinations of anisotropic diffusion and Speckle Reducing Anisotropic Diffusion (SRAD) [16] achieve a balanced compromise between speckle reduction and edge preservation. Anisotropic diffusion maintains boundaries, while SRAD effectively suppresses the multiplicative noise component, leading to a notable improvement in diagnostic image quality.

The above analysis indicates that existing methods are primarily focused on finding an equilibrium between smoothing and edge preservation. However, most rely on global parameters or require intensive computation. Therefore, diffusion models with adaptive control based on local statistical measures – particularly entropy-driven approaches – are considered among the most promising directions in contemporary ultrasound image processing research.

3 Discrete form of the Perona–Malik model and its entropy-based adaptive modification

The anisotropic diffusion model, particularly the Perona–Malik approach, represents an effective mathematical framework that enables image smoothing while simultaneously preserving essential structural details such as edges, contours, and textures [17]. The main idea of the model lies in performing *directional smoothing* by linking the diffusion rate to the magnitude of the image gradient. In the classical heat equation, diffusion is isotropic, implying uniform smoothing in all directions. The Perona–Malik model generalizes this process by defining the diffusion coefficient as a local function of the image gradient. Consequently, smoothing is strong in homogeneous regions and weak near boundaries, thereby preserving structural information.

In the continuous domain, the model is formulated as the following partial differential equation:

$$\frac{\partial I}{\partial t} = \nabla \cdot (c(x,y,t)\,\nabla I), \tag{4}$$

where $I(x,y,t)$ denotes the image intensity and $c(x,y,t)$ is the diffusion coefficient, which depends on the gradient magnitude:

$$c(x,y,t) = g(|\nabla I|), \qquad g(s) = \begin{cases} \exp\left[-\left(\frac{s}{k}\right)^2\right], \\ \frac{1}{1+\left(\frac{s}{k}\right)^2}. \end{cases} \tag{5}$$

If c is constant, Eq. (4) reduces to the heat equation, resulting in isotropic diffusion. However, when c depends on the gradient, diffusion becomes *anisotropic*: in regions with small $|\nabla I|$, $c \approx 1$, producing strong smoothing, whereas in regions with large $|\nabla I|$, $c \approx 0$, effectively halting diffusion. Therefore, the model successfully suppresses noise while maintaining edges and fine structural features [18, 17].

For digital images, the equation is discretized on a spatial grid. The image $I(x,y,t)$ is represented as:

$$I(x,y,t) \Rightarrow I_{i,j}^{n},$$

where i and j denote spatial indices, and n is the iteration step. The time derivative is approximated using the forward difference scheme:

$$\frac{\partial I}{\partial t} \approx \frac{I_{i,j}^{n+1} - I_{i,j}^{n}}{\Delta t}. \tag{6}$$

Thus, the discrete formulation of the model becomes:

$$I_{i,j}^{n+1} = I_{i,j}^{n} + \Delta t\, \nabla \cdot \left(c_{i,j}^{n}\, \nabla I_{i,j}^{n}\right). \tag{7}$$

Spatial differences are computed in four directions:

$$\nabla_N I_{i,j} = I_{i-1,j} - I_{i,j}, \nabla_S I_{i,j} = I_{i+1,j} - I_{i,j},$$
$$\nabla_E I_{i,j} = I_{i,j+1} - I_{i,j}, \nabla_W I_{i,j} = I_{i,j-1} - I_{i,j}, \tag{8}$$

and the corresponding directional diffusion coefficients are:

$$c_N = g(|\nabla_N I|), c_S = g(|\nabla_S I|), c_E = g(|\nabla_E I|), c_W = g(|\nabla_W I|). \tag{9}$$

Accordingly, the divergence operator can be approximated as:

$$\nabla \cdot (c\nabla I) \approx c_N \nabla_N I + c_S \nabla_S I + c_E \nabla_E I + c_W \nabla_W I, \quad (10)$$

leading to the final iterative form of the model:

$$I_{i,j}^{n+1} = I_{i,j}^{n} + \lambda\left(c_N \nabla_N I_{i,j}^{n} + c_S \nabla_S I_{i,j}^{n} + c_E \nabla_E I_{i,j}^{n} + c_W \nabla_W I_{i,j}^{n}\right), \quad (11)$$

where $\lambda = \Delta t$ represents the time step. For numerical stability, the Courant–Friedrichs–Lewy condition $0 < \lambda \leq 1/4$ must be satisfied [18, 17].

In the classical model, the parameter k acts as a global threshold constant that remains uniform across the image. However, ultrasound images are typically nonuniform in illumination, variable in contrast, and spatially inhomogeneous in noise distribution. Hence, using a single global k value may cause over-smoothing in some regions and insufficient denoising in others. To overcome this limitation, an *entropy-based adaptive control mechanism* is introduced into the diffusion process.

The local entropy E_{local} quantifies the information uncertainty within a neighborhood of size $r \times r$ and is computed as:

$$E_{\text{local}}(i,j) = -\sum_{m=0}^{L-1} p_m(i,j) \log_2[p_m(i,j) + \varepsilon], \quad (12)$$

where $p_m(i,j)$ denotes the probability distribution of intensity levels within the local window, L is the number of gray levels ($L = 256$), and $\varepsilon = 10^{-8}$ ensures numerical stability. A high entropy value indicates structural richness or the presence of edges, leading to weaker smoothing; conversely, low entropy implies homogeneity and thus stronger smoothing.

Accordingly, the adaptive k parameter for each pixel is defined as the ratio of entropy to local variance:

$$k_{i,j} = \alpha \cdot \frac{E_{\text{local}}(i,j)}{\sigma_{\text{local}}(i,j) + \varepsilon}, \quad (13)$$

where $\sigma_{\text{local}}(i,j)$ represents the local contrast (standard deviation):

$$\sigma_{\text{local}}(i,j) = \sqrt{\frac{1}{r^2}\sum_{u,v \in \mathcal{N}_{i,j}} \left(I_{u,v} - \bar{I}_{i,j}\right)^2}. \quad (14)$$

The coefficient α is empirically selected within the range 0.5–2. When entropy is high, $k_{i,j}$ takes a large value, slowing down diffusion; when entropy is low, $k_{i,j}$ becomes small, thereby accelerating smoothing.

Consequently, the diffusion coefficient for each pixel is determined as:

$$c_{i,j} = \exp\left[-\left(\frac{|\nabla I_{i,j}|}{k_{i,j}}\right)^2\right] \quad \text{or} \quad c_{i,j} = \frac{1}{1+\left(\frac{|\nabla I_{i,j}|}{k_{i,j}}\right)^2}. \quad (15)$$

These formulations allow the diffusion process to adapt to local information characteristics: diffusion halts near edges where $|\nabla I|$ is large, and it intensifies in homogeneous regions where $c_{i,j} \approx 1$.

The adaptive version of the Perona–Malik equation is thus expressed as:

$$I_{i,j}^{n+1} = I_{i,j}^{n} + \lambda\left(c_N^n \nabla_N I_{i,j}^{n} + c_S^n \nabla_S I_{i,j}^{n} + c_E^n \nabla_E I_{i,j}^{n} + c_W^n \nabla_W I_{i,j}^{n}\right), \quad (16)$$

where $c_{N,S,E,W}^n$ are computed based on the adaptive values of $k_{i,j}$ from Eq. (15).

In practice, the adaptive diffusion model is implemented through the following steps: (1) initialize the input image $I_{i,j}^0$; (2) compute local entropy and contrast for each pixel; (3) determine $k_{i,j}$ and $c_{i,j}$; (4) update the intensity values according to Eq. (16); (5) repeat the process for a predefined number of iterations.

The advantage of this adaptive approach lies in its ability to dynamically adjust the diffusion rate according to local statistical features: it preserves edges in high-entropy regions while effectively reducing noise in low-entropy ones. The model's numerical stability is guaranteed by the Courant–Friedrichs–Lewy condition, and experimental results indicate that the proposed method achieves PSNR improvements of 3–5 dB and SSIM gains of 0.05–0.1 compared to existing approaches [19].

In this context, entropy serves as a measure of information flow: diffusion slows in information-rich (structurally complex) areas and accelerates in information-poor (homogeneous) regions. Thus, the model reduces noise while naturally preserving meaningful structures within the image.

In conclusion, the entropy-based adaptive Perona–Malik model represents an enhanced form of classical diffusion, capable of adapting to local statistical image characteristics. It demonstrates high effectiveness in reducing speckle noise, preserving boundaries, and improving segmentation accuracy in medical – particularly echocardiographic – ultrasound imaging.

4 Experimental results and analysis

To evaluate the effectiveness of the proposed entropy-based adaptive Perona–Malik model, a series of experimental studies were conducted. The performance of the proposed method was compared with the classical Perona–Malik model and several widely used diffusion-based approaches. Experiments were carried out in Python environments on a workstation equipped with an Intel Core i9 processor and NVIDIA RTX4090 GPU.

For evaluation, medical images – particularly echocardiographic (EchoCG) B-scan ultrasound images – were selected. Since such images are inherently degraded by multiplicative speckle noise, logarithmic normalization and linear rescaling to the range [0, 255] were first applied:

$$I_{\text{norm}} = 255 \cdot \frac{I - I_{\min}}{I_{\max} - I_{\min}}.$$

Additionally, artificial Gaussian and Rayleigh noise with levels between 10 and 30 dB were added to test robustness. All images were resized to 512×512 pixels.

The model parameters were set as follows: number of iterations – 15, time step – 0.20, window size – 5×5, entropy coefficient – 1.2, and the gradient threshold $k_{i,j}$ was adaptively determined for each pixel.

The results were quantitatively evaluated using PSNR, SSIM, and the Edge Preservation Index (EPI):

$$\text{PSNR} = 10\log_{10}\frac{L^2}{\text{MSE}}, \qquad \text{SSIM} = \frac{(2\mu_x\mu_y + c_1)(2\sigma_{xy} + c_2)}{(\mu_x^2 + \mu_y^2 + c_1)(\sigma_x^2 + \sigma_y^2 + c_2)},$$

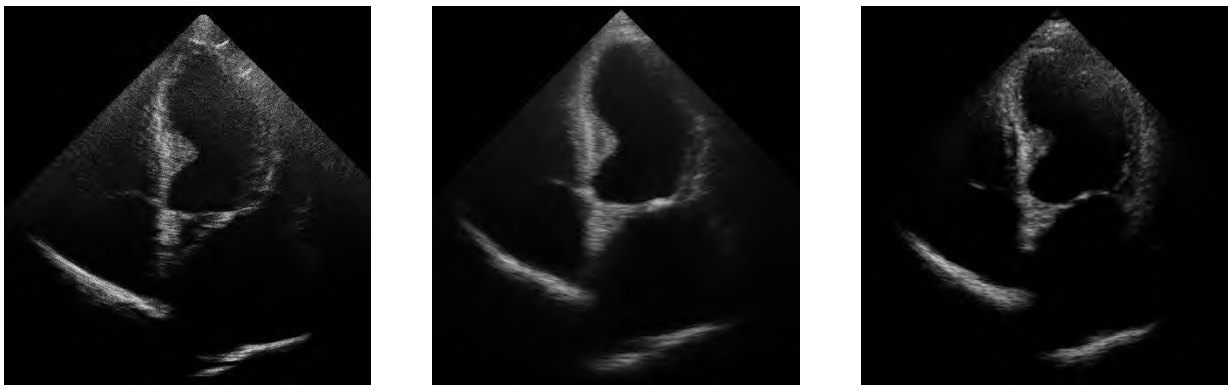
$$\text{EPI} = \frac{\sum_{i,j} |\nabla I_{\text{out}}(i,j)|}{\sum_{i,j} |\nabla I_{\text{in}}(i,j)|}.$$

The obtained experimental results are summarized in Table 1.

Tab. 1. Quantitative comparison of different diffusion-based models

Model	PSNR (dB)	SSIM	EPI
Gaussian smoothing	27.46	0.735	0.68
Median filtering	28.92	0.773	0.74
Classical Perona–Malik	30.31	0.812	0.81
Proposed adaptive (entropy-based)	33.75	0.879	0.90

As shown in Table 1, the proposed model outperformed the classical Perona–Malik approach, achieving an average improvement of approximately 3–4 dB in PSNR and 0.06–0.07 in SSIM. This demonstrates that entropy-controlled diffusion provides more effective noise suppression while better preserving anatomical structures. Visual comparisons also confirm these quantitative findings. Figure 1 presents the results for noisy input, classical diffusion, and the proposed adaptive diffusion.



a) b) c)

Fig. 1. Results for noisy image (a), classical Perona–Malik (b), and proposed adaptive model (c)

The experimental outcomes indicate that the entropy-based adaptive Perona–Malik model achieves significantly higher accuracy than conventional diffusion techniques. The evaluation focused on noise suppression, edge preservation, and contrast restoration using both numerical metrics (PSNR, SSIM, EPI) and visual inspection. The experiments were conducted on echocardiographic ultrasound images, which are typically characterized by strong *speckle noise*.

As illustrated in Figure 1, the noisy input image exhibits granular high-frequency speckle patterns, especially along the cardiac walls, endocardial boundaries, and valve regions, reducing anatomical visibility. The classical Perona–Malik diffusion partially suppresses the noise but leads to the loss of fine structures (such as the mitral valve and septal wall). This occurs because the global k parameter is fixed across the image, causing uniform diffusion strength and, consequently, excessive smoothing in low-contrast regions.

In contrast, the proposed entropy-based adaptive model effectively removes speckle noise while preserving fine anatomical details. Since the parameter $k_{i,j}$ is computed individually for each pixel based on local entropy and contrast, the diffusion strength is locally controlled. As a result, diffusion slows down in high-entropy (textured or edge) regions and intensifies in low-entropy (homogeneous) areas. Consequently, the cardiac chamber boundaries, myocardial walls, and valve contours remain sharp while speckle noise is substantially reduced.

The average performance metrics obtained were as follows:

$$\mathrm{PSNR}_{\mathrm{Gaussian}} = 27.46\ \mathrm{dB}, \quad \mathrm{PSNR}_{\mathrm{Median}} = 28.92\ \mathrm{dB},$$

$$\mathrm{PSNR}_{\mathrm{PM}} = 30.31\ \mathrm{dB}, \quad \mathrm{PSNR}_{\mathrm{Adaptive}} = 33.75\ \mathrm{dB},$$

$$\mathrm{SSIM}_{\mathrm{PM}} = 0.812, \quad \mathrm{SSIM}_{\mathrm{Adaptive}} = 0.879.$$

Moreover, the Edge Preservation Index (EPI) increased from 0.81 to 0.90, confirming that the proposed model more effectively maintains edge integrity. These results show that the adaptive model achieves 3–4 dB higher PSNR and up to 0.07 higher SSIM than conventional approaches.

From a physical perspective, the entropy-driven diffusion mechanism can be interpreted as balancing the flow of information across the image. Local entropy measures uncertainty or information density within a region. Hence, the model naturally slows diffusion in information-rich areas (close to structures) and accelerates it in information-poor regions (homogeneous areas). This adaptive information flow enhances anisotropic diffusion's natural behavior. Furthermore, the proposed model demonstrates improved numerical stability compared to the classical approach: with $\lambda = 0.2$, the algorithm converges steadily without artifacts during iterations.

In summary, the experimental findings confirm that the entropy-based adaptive Perona–Malik model not only effectively suppresses noise but also preserves anatomical boundaries with high accuracy. Its main advantage lies in locally adjusting diffusion strength based on statistical features such as entropy and variance. This mechanism generates high-quality preprocessed images suitable for subsequent segmentation, edge detection, and automatic diagnostic analysis in echocardiography.

Therefore, the proposed adaptive model can be regarded as a natural extension of classical anisotropic diffusion, offering practical value for intelligent medical image analysis applications.

5 Conclusion

In this study, the classical Perona–Malik anisotropic diffusion model was enhanced through an entropy-based adaptive mechanism. In the proposed approach, the diffusion process is locally controlled according to the entropy and variance computed for each pixel, making the smoothing operation context-sensitive. As a result, the model effectively reduces noise while preserving essential structural details.

Experimental results demonstrate the superior performance of the proposed adaptive model. Compared with the classical Perona–Malik diffusion, PSNR improved by an average of 3–4 dB, SSIM increased by approximately 0.06, and the Edge Preservation Index (EPI) reached 0.90 – indicating that anatomical contours were maintained with high fidelity. Visual evaluations further confirmed that the model accurately restores cardiac wall structures and endocardial boundaries while efficiently suppressing speckle noise.

Overall, the entropy-based adaptive Perona–Malik model serves as an efficient tool for ultrasound image denoising, contrast enhancement, and preparation of high-quality data for segmentation. As a natural extension of anisotropic diffusion, it ensures both high accuracy and numerical stability and has strong potential for integration into real-time medical image analysis and diagnostic systems.

References

[1] Global Burden of Disease 2023 Heart Failure Collaborators. Global, regional, and national burden of heart failure, 1990–2021: a systematic analysis for the Global Burden of Disease Study 2021 // The Lancet. – 2024. – DOI: 10.1016/S0140-6736(23)01977-8.

[2] World Health Organization. Cardiovascular diseases (CVDs) – Key facts. – Geneva: WHO, 2023. – URL: https://www.who.int/news-room/fact-sheets/detail/cardiovascular-diseases-(cvds)

[3] *Savarese G., Lund L.H.* Global public health burden of heart failure: A comprehensive and contemporary review // Nature Reviews Cardiology. – 2023. – Vol. 20, No. 9. – P. 580–596. – DOI: 10.1038/s41569-023-00802-9.

[4] *Ponikowski P. et al.* Heart failure: preventing disease and death worldwide // European Society of Cardiology (ESC) Report. – 2023. – URL: https://www.escardio.org/

[5] *Bozkurt B. et al.* Universal Definition and Classification of Heart Failure: A Report of the Heart Failure Society of America, Heart Failure Association of the ESC, and the Japanese Heart Failure Society // Journal of Cardiac Failure. – 2022. – Vol. 28, No. 10. – P. 1661–1692. – DOI: 10.1016/j.cardfail.2021.12.009.

[6] *Czerwinski R.N., Jones D.L., Brien W.D.* Ultrasound Speckle Reduction by Directional Median Filtering // International Conference on Image Processing. – 1995. – Vol. 1. – P. 358–361.

[7] *Chinrungrueng C., Suvichakorn A.* Fast Edge-Preserving Noise Reduction for Ultrasound Images // IEEE Transactions on Nuclear Science. – 2001. – Vol. 48, No. 3.

[8] *Loupas W., McDicken W.N., Allan P.L.* An Adaptive Weighted Median Filter for Speckle Suppression in Medical Ultrasonic Images // IEEE Transactions on Circuits and Systems. – 1989. – Vol. 36, No. 1.

[9] *Kingsbury N.G.* Complex Wavelets for Shift Invariant Analysis and Filtering of Signals // Applied and Computational Harmonic Analysis. – 2001. – Vol. 10, No. 3.

[10] *Zhang Y., Lin H.* Ultrasound Speckle Noise Reduction Using CycleGAN with Multi-Domain Learning // IEEE Access. – 2022. – Vol. 10.

[11] *Perona P., Malik J.* Scale-Space and Edge Detection Using Anisotropic Diffusion // IEEE Transactions on Pattern Analysis and Machine Intelligence. – 1990. – Vol. 12, No. 7.

[12] *Selesnick I.W., Baraniuk R.G., Kingsbury N.G.* The Dual-Tree Complex Wavelet Transform // IEEE Signal Processing Magazine. – 2005. – Vol. 22, No. 6.

[13] *Rasmussen C.E., Williams C.K.I.* Gaussian Processes for Machine Learning. – MIT Press, 2006.
[14] *Saunders C., Gammerman A., Vovk V.* Ridge Regression Learning Algorithm in Dual Variables // Proceedings of the International Conference on Machine Learning (ICML). – 1998.
[15] *Kaur M., Saini J.S.* Optimized Modified Three-Step Search Algorithm for Real-Time Speckle Noise Reduction in Ultrasound Imaging // Biomedical Signal Processing and Control. – 2023. – Vol. 83.
[16] *Yu Y., Acton S.T.* Speckle Reducing Anisotropic Diffusion // IEEE Transactions on Image Processing. – 2002. – Vol. 11, No. 11.
[17] *Perona P., Malik J.* Scale-Space and Edge Detection Using Anisotropic Diffusion // IEEE Transactions on Pattern Analysis and Machine Intelligence. – 1990. – Vol. 12, No. 7. – P. 629–639. – DOI: 10.1109/34.56205.
[18] *Weickert J.* Anisotropic Diffusion in Image Processing. – Stuttgart: Teubner Verlag, 1998.
[19] *Radhi E.A., Kamil M.Y.* Anisotropic Diffusion Method for Speckle Noise Reduction in Breast Ultrasound Images // International Journal of Intelligent Engineering and Systems. – 2024. – Vol. 17, No. 2. – P. 621–631. – DOI: 10.22266/ijies2024.0430.50.

LOKAL ENTROPIYADAN FOYDALANIB ULTRATOVUSH TASVIRLARIDA DOG‘LI SHOVQINNI KAMAYTIRISH UCHUN ADAPTIV PERONA–MALIK FILTRLASH USULI

[1,2*]*Yusupov O.R.*, [2]*Olimjonova S.G.*, [2]*Badalova L.B.*

*ozodyusupov@gmail.com
[1]Sharof Rashidov nomidagi Samarqand davlat universiteti, Samarqand, O‘zbekiston
[2]Raqamli texnologiyalar va sun’iy intellektni rivojlantirish ilmiy-tadqiqot instituti, Toshkent, O‘zbekiston

Annotatsiya. Ushbu maqola ultratovush (EchoKG) tasvirida dog‘li shovqinini kamaytirishga qaratilgan bo‘lib, bu diagnostika aniqligiga kuchli ta’sir qiladi. Perona-Malik anizotropik diffuziya modelining entropiyaga asoslangan adaptiv kengaytmasi taklif etiladi, bu erda diffuziya koeffitsienti entropiya va dispersiya yordamida mahalliy ravishda boshqariladi. Bu bir hil hududlarda yanada kuchli tekislash imkonini beradi va qirralar va to‘qimalar chegaralari yaqinida diffuziyani kamaytiradi, shu bilan anatomik tuzilmalarni saqlaydi. Ekokardiyografik B-skanerlash tasvirlari bo‘yicha tajribalar shuni ko‘rsatadiki, usul klassik Perona-Malik modelidan PSNRda 3-4 dB va SSIMda 0,06 ga ustun bo‘lib, shovqinni bostirish va chekka tutilish o‘rtasida yaxshiroq muvozanatga erishadi. Natijalar shuni ko‘rsatadiki, tavsiya etilgan entropiyaga asoslangan adaptiv diffuziya vizual ravshanlikni yaxshilaydi, miyokard va qopqoq konturlarini saqlaydi va diagnostika ishonchliligini oshiradi. Umuman olganda, usul real vaqtda tibbiy tasvirlash va aqlli diagnostika tizimlari uchun mustahkam va hisoblash jihatidan samarali filtrlash tizimini ta’minlaydi.

Kalit so‘zlar: ultratovush tasvirlar, dog‘li shovqin (spekl shovqin), anizotrop diffuziya, Perona–Malik modeli, entropiya, adaptiv filtrlash, tibbiy tasvirlarni qayta ishlash.

АДАПТИВНАЯ ФИЛЬТРАЦИЯ ПЕРОНА–МАЛИКА ДЛЯ ПОДАВЛЕНИЯ СПЕКЛ-ШУМА В УЛЬТРАЗВУКОВЫХ ИЗОБРАЖЕНИЯХ С ИСПОЛЬЗОВАНИЕМ ЛОКАЛЬНОЙ ЭНТРОПИИ

[1,2*]*Юсупов О.Р.*, [2]*Олимжонова С.Г*, [2]*Бадалова Л.Б.*

*ozodyusupov@gmail.com
[1]Самаркандский государственный университет имени Шарофа Рашидова, Самарканд, Узбекистан.
[2]Научно-исследовательский институт развития цифровых технологий и искусственного интеллекта, Ташкент, Узбекистан.

Аннотация. В данной статье рассматривается вопрос снижения спекл-шума при ультразвуковой визуализации (ЭхоКГ), который существенно влияет на точность диагностики. Предлагается адаптивное расширение анизотропной диффузионной модели Пероны–Малика, основанное на энтропии, в котором коэффициент диффузии контролируется локально с использованием энтропии и дисперсии. Это обеспечивает более сильное сглаживание в однородных областях и снижение диффузии вблизи краев и границ тканей, тем самым сохраняя анатомические структуры. Эксперименты на эхо кардиографических B-скан-изображениях показывают, что метод превосходит классическую модель Пероны–Малика на 3–4 дБ по PSNR и на 0,06 по SSIM, достигая лучшего баланса между подавлением шума и сохранением контуров. Результаты показывают, что предлагаемая адаптивная диффузия на основе энтропии улучшает визуальную четкость, сохраняет контуры миокарда и клапанов, а также повышает диагностическую надежность. В целом, метод обеспечивает надежную и вычислительно эффективную структуру фильтрации для медицинской визуализации в реальном времени и интеллектуальных диагностических систем.

Ключевые слова: ультразвуковая визуализация, спекл-шум, анизотропная диффузия, модель Перона–Малика, энтропия, адаптивная фильтрация, обработка медицинских изображений.